Changes in crop yields and their variability at different levels of global warming

Sebastian Ostberg[1,2], Jacob Schewe[1], Katelin Childers[1], Katja Frieler[1]

[1]Potsdam Institute for Climate Impact Research, Telegrafenberg A31, 14473 Potsdam, Germany
[2]Geography Department, Humboldt-Universität zu Berlin, Berlin, Germany

Abstract

An assessment of climate change impacts at different levels of global warming is crucial to inform the political discussion about mitigation targets, as well as for the economic evaluation of climate change impacts e.g. in economic models such as Integrated Assessment Models (IAMs) that internally only use global mean temperature change as indicator of climate change. There is already a well-established framework for the scalability of regional temperature and precipitation changes with global mean temperature change (ΔGMT). It is less clear to what extent more complex, biological or physiological impacts such as crop yield changes can also be described in terms of ΔGMT; even though such impacts may often be more directly relevant for human livelihoods than changes in the physical climate. Here we show that crop yield projections can indeed be described in terms of ΔGMT to a large extent, allowing for a fast interpolation of crop yield changes to emission scenarios not originally covered by climate and crop model projections. We use an ensemble of global gridded crop model simulations for the four major staple crops to show that the scenario dependence is a minor component of the overall variance of projected yield changes at different levels of ΔGMT. In contrast, the variance is dominated by the spread across crop models. Varying CO_2 concentrations are shown to explain only a minor component of the remaining crop yield variability at different levels of global warming. In addition, we show that the variability of crop yields is expected to increase with increasing warming in many world regions. We provide, for each crop model and climate model, patterns of mean yield changes that allow for a simplified description of yield changes under arbitrary pathways of global mean temperature and CO_2 changes, without the need for additional climate and crop model simulations.

1. Introduction

Climate change exerts a substantial and direct impact on food security and hunger risk by altering the global patterns of precipitation and temperature which determine the location of arable land (Parry *et al* 2005, Rosenzweig *et al* 2014) as well as the quality (Müller *et al* 2014) and quantity (Müller and Robertson 2014, Lobell *et al* 2012, van der Velde *et al* 2012) of crops comprising most of the world food supply. Climate change alone is expected to reduce global production of the four major crops wheat, maize, soy and rice on current agricultural areas (e.g., Rosenzweig *et al* 2014,

Challinor and Wheeler 2008, Peng *et al* 2004). Facing an increasing food demand due to population growth and economic development, these reductions will have to be overcompensated by 1) the direct physiological impacts of increased atmospheric CO_2 concentrations (Kimball 1983),

45 which are beyond local human control; as well as 2) advances in agricultural management (e.g. fertilizer input or irrigation), technology, and breeding (Jaggard et al 2010) or 3) expansion of agricultural land (Frieler et al 2015, Smith et al 2010).

In conjunction with these long term changes, global warming is also expected to contribute to an

50 increase in the frequency and duration of extreme temperatures and precipitation (droughts, floods, and heat waves), which may increase the near term variability of crop yields and trigger short term crop price fluctuations (Brown & Kshirsagar, 2015; Mendelsohn, Basist, Dinar, Kurukulasuriya, & Williams, 2007; Tadesse, Algieri, Kalkuhl, & von Braun, 2014).

55 The emission of greenhouse gases is expected to influence crop yields via several channels. On the one hand the associated climate changes will modify the length of the growing season (Eyshi Rezaei *et al* 2014), water availability, and heat stress (Lobell, Sibley, & Ivan Ortiz-Monasterio, 2012; Müller & Robertson, 2014; Schlenker & Roberts, 2009); and on the other hand higher concentrations of atmospheric CO_2 are expected to increase the water use efficiency in C3 (e.g.

60 wheat, rice, soy) and C4 (maize) crops, and enhance the rate of photosynthesis in C3 crops (Darwin and Kennedy 2000). Global Gridded Crop Models (GGCMs) are particularly designed to account for these effects. They provide a complex process-based implementation of our current understanding of the mechanisms underlying crop growth, and are the primary tool for crop yield projections (e.g., Rosenzweig *et al* 2014) which in turn are a prerequisite for assessing potential

65 changes in prices (Nelson *et al* 2014) and food security (Parry *et al* 2005).

However, these process-based crop yield projections rely on spatially explicit realizations of the driving weather variables such as temperature, precipitation, radiation, and humidity, often at daily resolution, as provided by computationally expensive Global Climate Model (GCM)

70 simulations. The GGCMs themselves also require significant computational capacity. These requirements generally limit the number and duration of emission scenarios that can be considered. The so-called pattern scaling approach is a well-established method to overcome these limits. Output from GCMs has been shown to be, to some extent, scalable to different global mean temperature (GMT) trajectories not originally covered by GCM simulations (Santer, Wigley,

75 Schlesinger, & Mitchell, 1990, Carter, Hulme, & Lal, 2007, Mitchell 2003, Giorgi 2008, Solomon *et al* 2009, Frieler *et al* 2012, Heinke *et al* 2013). Scaled climate projections have also been used as input for different impact models (Ostberg et al 2013, Stehfest et al 2014) to gain flexibility with regard to the range of emission scenarios considered.

80 Building upon such a framework, we present a method to extend the capacity of crop yield impact projections by relating simulated crop yields to two highly aggregated quantities – global mean temperature change (ΔGMT) and atmospheric CO_2 concentration (pCO2) – by means of simplified function. ΔGMT and pCO2 are the standard output of simple climate models, which allow for highly efficient climate projections for any emissions scenario by emulating the response of the

85   complex GCMs (Meinshausen *et al* 2011). Here "emulating" means that the simplified
representation is designed to reproduce the complex model response for the originally simulated
scenarios but allows for its inter- or extrapolation to other scenarios. In this way our approach is
different from other emulators building on regional explicit climate projections as input for the
simplified functions emulating complex crop models' responses to these forcings (Blanc, 2017).
90   While these approaches only emulate the crop model responses, the approach presented here
implicitly provides a simplified description of the GCMs' regional patterns of climate change and
the associated response of the crop models.

We test to what extent climate change impacts such as crop yields can be directly described in
95   terms of GMT (and pCO_2) changes without an intermediate scaling of the regional climate changes.
Such a direct description of the simulated impacts – in contrast to scaling the climate changes for
specific emission scenarios and then using the scaled climate projections as input for impact
model simulations – has the advantage of saving computation time, making the approach e.g.
applicable within Integrated Assessment Models and even when no impact model is accessible. In
100   principle, scaled but spatially explicit climate projections could also be used as input for spatial
explicit crop model emulators (Blanc, 2017) to reach high efficiency. However, in this case the
scaling of the climate information has to be carefully adjusted to provide the kind of climate
information required by the impact model impact emulator and this two-step approach also mean
two approximations that may lead to higher deviations than the one-step approach proposed
105   here.

The emulator introduced here allows for multi-impact-model projections for arbitrary emission
scenarios as long as ensemble projections are available for a limited set of scenarios. This offers a
practical way of keeping track of a relevant but often-ignored source of uncertainty which is
110   manifested in the considerable spread across different crop models and other process-based
impact models (Rosenzweig *et al* 2014, Schewe *et al* 2014). This uncertainty is particularly critical
when estimating socio-economic consequences (e.g., Nelson *et al* 2014).

We test the approach using an ensemble of yield projections of the four major cereal crops (maize,
115   rice, soy, and wheat), generated within the first phase ("Fast Track") of the Inter-sectoral Impact
Model Intercomparison Project (ISIMIP, Warszawski et al., 2014). For a number of ΔGMT intervals
we compare the spread in yield outcomes induced by the choice of emission scenario with that
induced by the choice of GGCM and GCM, respectively. A low scenario-induced spread means that
GCM- and GGCM-specific yield projections can be approximated by a simplified relationship with
120   global mean temperature change without accounting for the underlying emission scenario. The
test is done at each grid cell and separately for simulations of purely rain-fed yields and fully
irrigated yields. Multi-model ensembles of crop yields over such a wide range of crops, CO_2
concentrations, and irrigation options are a new prospect and the ISIMIP data provides a uniquely
broad suite of crop yield impact simulations encompassing output from five GGCMs, forced with
125   output from up to five GCMs, and four Representative Concentration Pathways (RCPs, van Vuuren
et al 2011a).

In Section 2 we describe the ISIMIP data and the methods used to test for scenario dependence and adjustment for different levels of CO$_2$. Section 3 is dedicated to the presentation of the projected average changes in crop yields at different levels of global warming and an attribution of the variance of these long term changes to different sources of uncertainty, i.e., different GCMs, different GGCMs, and different emission scenarios (Section 3.1). The simulated impacts of climate and CO$_2$ changes on global and regional crop yields are shown to be related to global mean temperature change, and to be largely independent of the emissions scenario. In addition, we test to what degree the scenario-dependence of crop yields at different levels of global warming can be explained by different levels of CO$_2$ (section 3.2).   Thus, finally we provide individual maps of yield changes at different levels of global mean temperature and the additional effect of variations in CO$_2$ concentration at given global mean temperature levels. We propose three methods to generate these patterns based on the available complex model simulations, and describe the related approaches to estimate GGCM- and GCM-specific yield changes for new ΔGMT trajectories not originally covered by GCM-crop-model simulations. In section 4 we present a quantification of the projection errors as compared to actual simulations by the complex gridded crop model. Finally, in section 5 we quantify the residual variance of the simulated crop yields in terms of global mean temperature change for each combination of crop and climate models. Section 6 provides a summary.

2. Data and Methods

We use projections from five different GGCMs (GEPIC, LPJ-GUESS, LPJmL, PEGASUS, and pDSSAT) that participated in in the first simulations round of ISIMIP (Rosenzweig *et al* 2014, Warszawski *et al* 2014) in order to test for a dependence of projected yield changes on the global mean temperature pathway (see Table 1 for their basic characteristics). Each crop model was forced by climate projections of five different GCMs (HadGEM2-ES, IPSL-CM5A-LR, MIROC-ESM-CHEM, GFDL-ESM2M, NorESM1-M) generated for four RCPs in the context of the Coupled Model Intercomparison Project, phase 5 (CMIP5). Climate projections have been bias-corrected to better match observed historical averages of the considered climate variables (Hempel *et al* 2013). Separate simulations are available for each of the four major crops: wheat, maize, rice and soy, on a global 0.5 x 0.5 degree grid. The considered crop is assumed to grow everywhere on the global land area, only restricted by soil characteristics and climate but independent of present or future land use patterns ("pure crop" simulations). Each model has provided a pair of simulations ("runs") for each climate change scenario: 1) a rain-fed run and 2) a full-irrigation run assuming no water constraints. This design provides full flexibility with regard to the application of future land use and irrigation patterns. While the "default" crop yield simulations (Y$_{CO2}$) account for the fertilization effects due to the increasing levels of atmospheric CO$_2$, the ISIMIP setting also includes a sensitivity experiment where the impact models were forced by climate change projections from HadGEM2-ES, RCP8.5 but CO$_2$ concentration was kept fixed at a "present day" reference level that differs from GGCM to GGCM (see Table 1). We will refer to this run as "fixed CO$_2$" run and indicate the associated crop yields by Y$_{noCO2}$.

170

Table 1: Basic crop model characteristics with respect to 1) the implementation of CO_2 fertilization effect (as affecting radiation use efficiency (RUE), transpiration efficiency (TE), leaf level photosynthesis (LLP), or canopy conductance (CC)), 2) the accounting for nutrient constraints with

175 respect to the CO_2 fertilization effect and associated assumption with respect to fertilizer application (N = nitrogen, P = phosphorus, K = potassium), 3) implemented adaptation measures, and 4) starting conditions.

model	CO_2 fertilization	Fertilizer use	Adaptation	Starting conditions
GEPIC (Liu, Williams, Zehnder, & Yang, 2007; Liu, 2009)	RUE, TE pCO₂ of the fixed CO_2 run: 364 ppm	Limitation of potential biomass increase due to N stress (flexible N application based on N stress >10% up to an upper national application limit according to FertiStat (FAO, 2007)) Fixed present day P application rates following FAO FertiStat database (FAO, 2007)	decadal adjustment of planting dates; total heat units to reach maturity remain constant decadal adjustment of winter and spring wheat sowing areas based on temperature	present day
LPJ-GUESS (Lindeskog, Arneth, Bondeau, Waha, Seaquist, et al., 2013)	LLP, CC pCO₂ of the fixed CO_2 run: 379 ppm	no consideration of spatial and temporal changes in nutrient limitation	cultivar adjustments are represented by variable heat units to reach maturity (Lindeskog, Arneth, Bondeau, Waha, Schurgers, et al., 2013), adjustments are based on the average climate over the preceeding 10 years	uncalibrated

LPJmL (Bondeau et al., 2007)	LLP, CC pCO₂ of the fixed CO₂ run: 370 ppm	soil nutrient limiting factors are not accounted for	fixed sowing dates (Waha, van Bussel, Müller, & Bondeau, 2012), total heat units to reach maturity remain constant	present day (Leaf Area Index (LAI), the Harvest Index (HI), and a scaling factor that scales leaf-level photosynthesis to stand level are adjusted to reproduce observed yields on country levels.)
PEGASUS (Deryng, Sacks, Barford, & Ramankutty, 2011)	RUE, TE pCO₂ of the fixed CO₂ run: 369 ppm	fixed N, P, K application rates (IFA, 2002)	adjustment of planting dates, variable heat units to reach maturity	present day
pDSSAT	RUE, LLP, CC pCO₂ of the fixed CO₂ run: 330 ppm	fixed N present day application rates	no adjustment of planting dates; total heat units to reach maturity remain constant	present day

180

For the analysis of the gridded data, rain-fed and full-irrigation simulations for each crop are considered separately. Considering e.g., wheat yield changes under full irrigation, we group all available data into ΔGMT intervals (bins) separated by 0.5°C steps with 0.5°C width (±0.25°C), where ΔGMT is relative to the present day (1980-2010 average) reference level. For all annual data

185 falling into a given interval and at one specific grid point we apply a separate one-way analysis of variance (ANOVA fixed effects model) to individually calculate the variance explained by 1) different GGCMs, 2) the GCMs, and 3) the RCPs. The quantification of the RCP-dependence of the relationship between global warming and yield changes is limited to a warming range up to 3°C above present because only one RCP (RCP8.5) reaches temperatures above this threshold.

190 However, we also provide the patterns of yield changes for the higher concentration scenario. In the main text all figures except Figure 1 refer to a ΔGMT level of 2.5°C (see Figure 1 for the associated years included) but the Supplement contains the figures for the other levels.
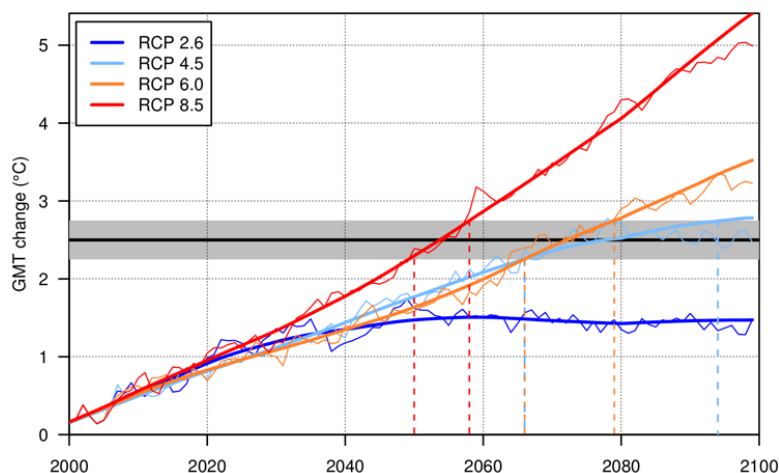
195

Figure 1. GMT projections from HadGEM2-ES for the four RCPs. The horizontal line and shading indicate the 2.5°C bin. The original annual GMT values (thin lines) are smoothed (thick lines) in order to obtain a contiguous time interval for each ΔGMT bin. The smoothing is based on a Singular Spectrum Analysis with a time window of 20 years (R-Package Rssa). E.g., years where the

200 thick line falls within the shaded area are associated with ΔGMT=2.5°C, and the corresponding time interval is delineated by the dashed vertical lines.

205 We do not impose a specific functional relationship between global mean temperature change and changes in crop yields. Yield changes for any global mean temperature level between the central levels of the considered bins could be derived by a simple linear interpolation between the patterns of neighboring bins but without assuming a linear relationship between global mean warming and yield changes across the full range of warming.

210

The direct effect of CO_2 fertilization on crop yields is expected to introduce some scenario dependence in the relationship between global mean temperature change and yield changes. We test to what degree the scenario dependence of the relationship can be explained by introducing atmospheric CO_2 levels as an additional predictor for within-bin fluctuation of yields. To this end,

215 we evaluate two different approaches to estimate the direct CO_2 effect on crop yields within the different global mean temperature bins, described in detail in Section 3.2

To evaluate and compare the performance of the two approaches we consider large scale regional average yields based on fixed present day (1998-2002) land use and irrigation patterns from

220 MIRCA2000 (Portmann *et al* 2010) and assess the reproducibility of the original RCP2.6, RCP4.5, and RCP6.0 projections based on the emulated yield patterns (section 4).

3. Mean Yield Change with Global Mean Temperature Change

225 ## 3.1 Patterns of relative changes at different levels of global warming and main sources of variance

In general, increasing global mean temperatures correspond to an expansion of arable land to higher latitudes with concurrent yield reductions in equatorial regions. The highest positive
230 changes in projected yields under rain-fed conditions at 2.5°C ΔGMT are typically in the northern high latitudes and mountainous regions for all crops (Figure 2). These locations were previously inhibited by a short growing season, which extends with increasing air temperature (Ramankutty *et al* 2002). Yield gains also occur over previously moisture limited regions, such as the northwestern U.S. and north-eastern China, in agreement with the findings of Ramankutty et al
235 (2002). In contrast, near the equator most crop yields decrease, especially maize and wheat. Since most cultivated land currently lies in low and middle latitudes, potential yield changes in those regions contribute a higher relative importance for today's food production system than changes in high latitudes.

240
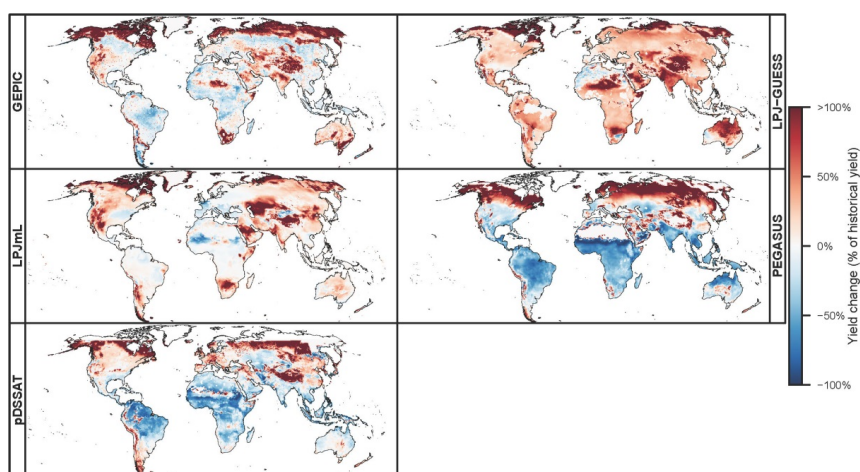
245 **Figure 2.** Average potential wheat yield change at ΔGMT=2.5°C as a percentage of the mean historical yield (1980-2010 average) under rain-fed conditions for each crop model forced by HadGEM2-ES. The average is calculated across all RCPs which reach the global mean warming interval from 2.25 to 2.75°C, namely RCP4.5, RCP6.0, and RCP8.5. Note that pDSSAT is run over a limited domain excluding areas north of 60°N. Analogous figures for different crops, for irrigated
250 conditions, as well as for absolute yield change (in t/ha) are available as supplementary online material.

While variations exist in the magnitude of projected yield changes, there is a high degree of

consistency in the direction of yield change across ensemble members, especially over the high
255 latitudes, where most of the largest projected yield changes occur, but where yields are in general
smaller (Figure 3). Utilizing output from all available combinations of one GCM, GGCM, and RCP
scenario, more than three-quarters of the ensemble members indicate increasing crop yields over
the upper mid latitudes in the northern hemisphere for all crops at 2.5°C.

260

265

270

275
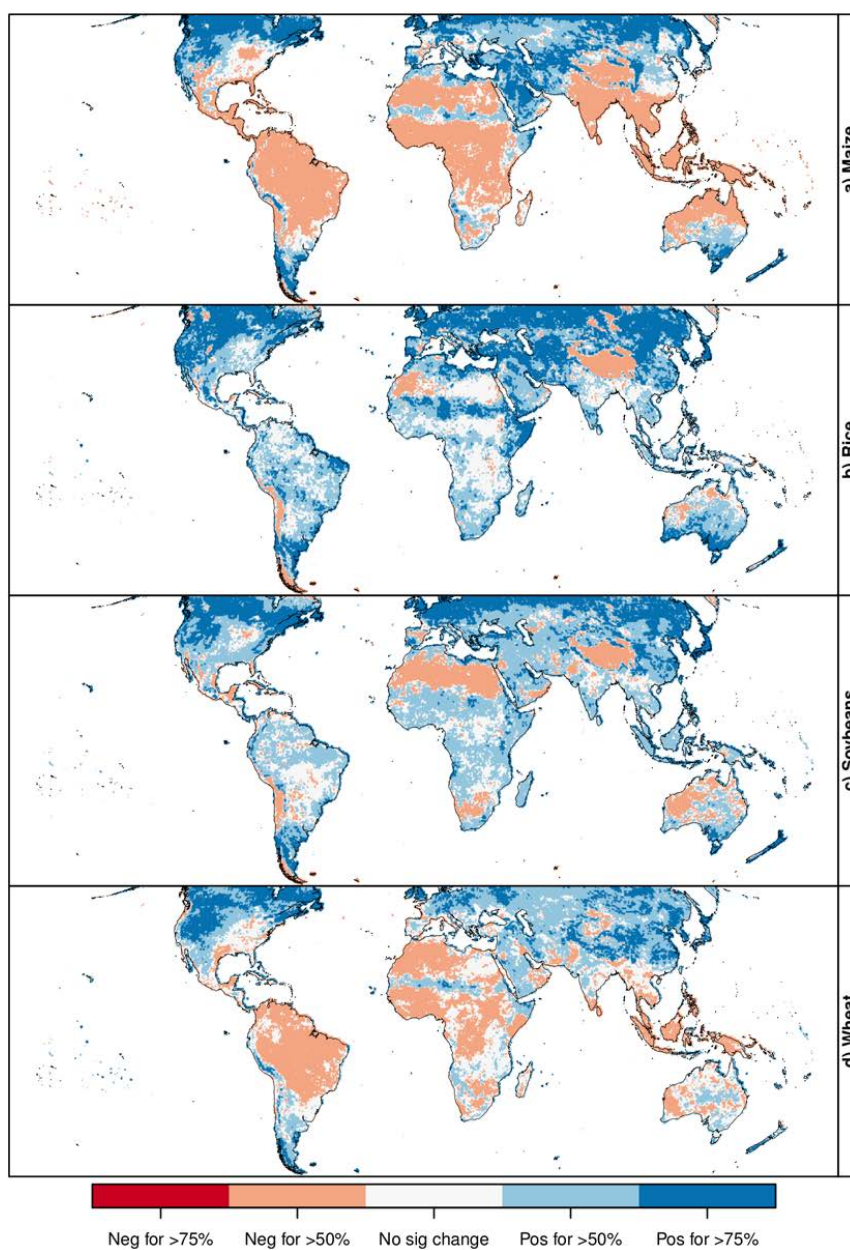
280

Figure 3. Percentage of crop model simulations (combination of a single GCM, GGCM, and RCP scenario) indicating an increase (blue) or decrease (red) in yield of greater than 5% at each grid point at 2.5°C warming scenario as compared to the historic period for a) maize, b) rice, c) soybeans, and d) wheat under rain-fed conditions. White indicates either a less than 5% change or disagreement between the models in the direction of yield change. An analogous figure for irrigated conditions is available as supplementary online material.

The simulated yield values at each grid point and within each GMT bin are subject to variation due
290   to the selection of impact model, GCM forcing, and emissions scenario. When considering all of
these factors, the variance attributable to the impact model selection is much greater than that
associated with the GCM or scenario choice in most regions (Figure 4). This holds for rainfed as
well as irrigated simulations and at all global mean warming bins above 1°C. The predominance of
the impact model component in total variance is particularly evident in the middle to high
295   latitudes for all four cereal crops, where impact model variance accounts for up to 90% of the grid
point variance at 2.5°C.
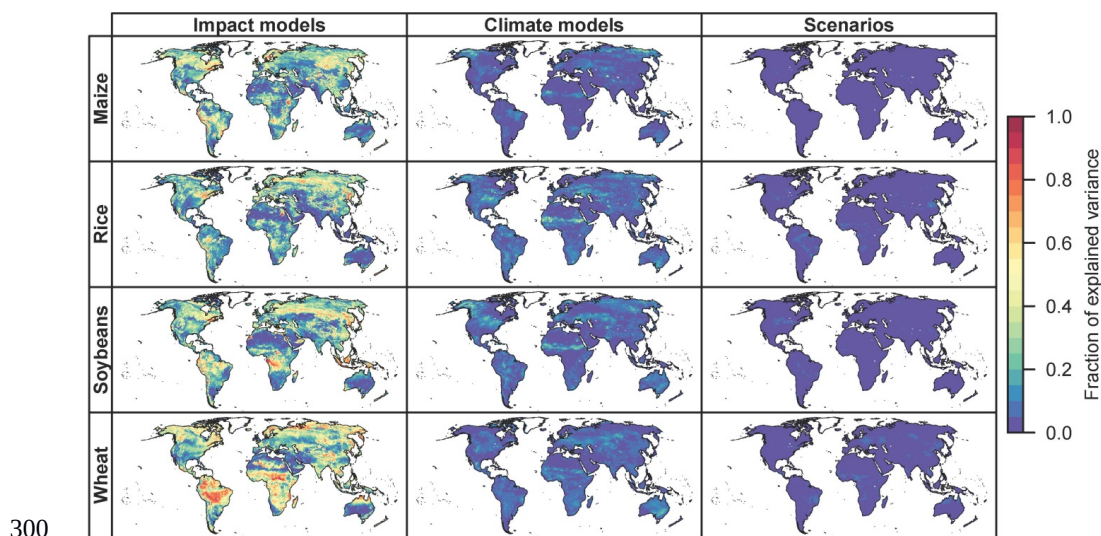
300

Figure 4. Fraction of total variance attributable to the impact models (GGCMs, left), climate
models (GCMs, middle), and scenarios (RCPs, right) for each crop. Figure shown for rain-fed runs
at ΔGMT=2.5°C warming; an analogous figure for irrigated runs is provided as supplementary
305   online material.

3.2 Direct impacts of increasing pCO2

In addition to air temperature warming, pCO2 has a direct influence on crop yields. As it varies
310   within the different ΔGMT bins, it is expected to induce part of the fluctuations of the yield
changes at given GMT levels. We find that this CO2 effect is not scenario dependent (see Figure 5
for the global average effect within the LPJmL simulations), consistent with a short response time
of plants to pCO2 changes.

315
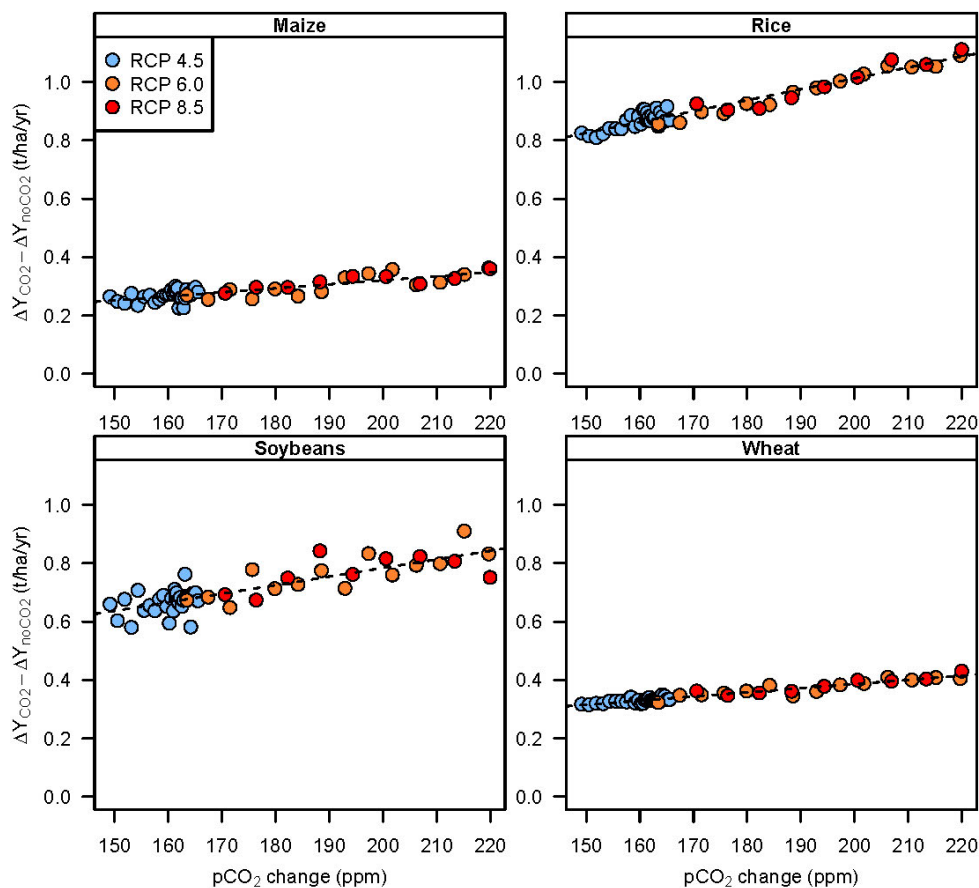
Figure 5. Difference in global mean yield change (sum of rainfed and irrigated, and weigthed by present-day growing areas) between the default (Y_{CO2}) and fixed CO2 simulations (Y_{noCO2}), for each crop over the range of pCO2 associated with the ΔGMT =2.5°C bin. Results are as simulated by LPJmL forced with output from HadGEM2-ES. Each color represents an emission scenario and black dotted lines indicate the linear best fit for each crop.

320

As expected, the differences increase with heightened atmospheric CO2 level under all emissions scenarios, implying a stronger CO2 fertilization impact with increased pCO2. A least squares fit to the yield differences versus greenhouse gas level within each ΔGMT bin allows for a quantification of the direct CO2 effect at each level of warming based on global pCO2, rather than the emissions pathway. The underlying assumption is that the effect of the temperature variation within the 0.5°C range of each ΔGMT bin will be minimal compared to the effect of the CO2 variation across all RCPs.

325

330

To quantify the extent of the CO2 induced scenario dependence and its potential reduction at each grid point, we use two methods to determine the CO2 effect on crop yields within each global mean temperature bin:

335

(a) By linear regression of absolute yield changes with respect to the historical reference period (ΔY_{CO2}) on CO_2 concentration within the individual global mean warming bins, i.e. by fitting the following model

340
$$\Delta Y_{CO2,\,i} = \Delta Y_{CLIM} + a_1 * (pCO_{2,\,i} - 370\ ppm) + \varepsilon_i, \qquad (1)$$

where i indicates the individual year within the relevant ΔGMT bin, and $\varepsilon_i \sim N(0, \sigma^2)$ represents the residual error. The statistical model allows for the estimation of the purely climate-induced yield change ΔY_{CLIM} at a fixed year-2000 concentration of CO2 of 370 ppm.

345

(b) By linear regression of the within-bin differences between the default crop simulations (Y_{CO2}) and the fixed CO2 run (Y_{noCO2}) on the underlying CO2 concentration in the default simulation:

$$(Y_{CO2,\,i} - Y_{noCO2,\,i}) = a_0 + a_1 * (pCO_{2,i} - 370\ ppm) + \varepsilon_{i,} \qquad (2)$$

350

where i indicates the individual year and $\varepsilon_i \sim N(0, {}^2)$ represents the residual error. In this case the purely climate-induced yield change $\Delta Y_{CLIM}(\Delta GMT)$ is given by the yield change in the fixed CO2 run, $\Delta Y_{noCO2}(\Delta GMT)$, and an additive correction a_0. This correction accounts for the different levels of pCO2 in the fixed-CO2 run across different models; it is zero if the pCO2 in
355 the fixed-CO2 run is 370 ppm.
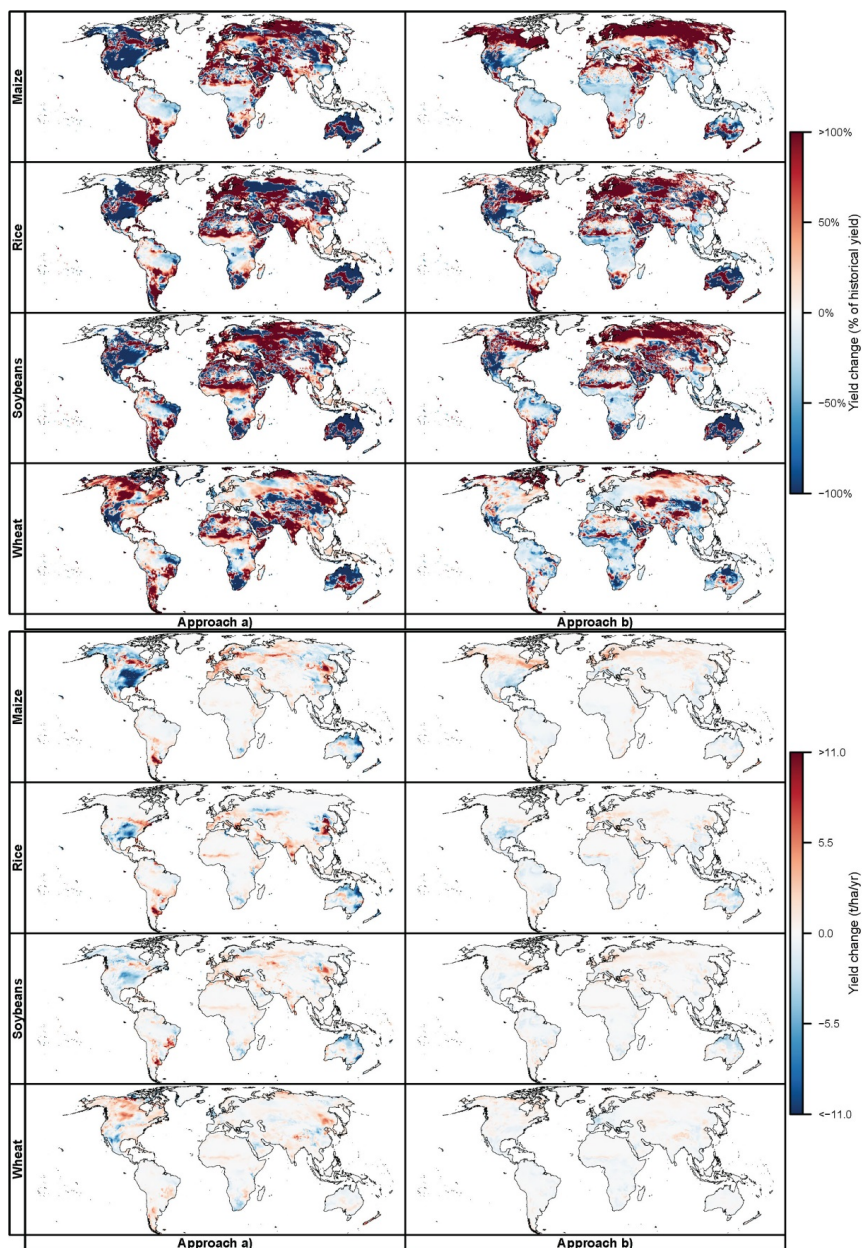
Figure 6. Climate change-induced yield changes at ΔGMT= 2.5°C of global warming and year 2000 pCO2 level (370ppm). Left column: Patterns of ΔY_{CLIM} derived at each grid point by method (a) (see equation (1)). Right column: Patterns of $\Delta Y_{noCO2}(2.5°C)+ a_0$, derived by method (b) (see equation (2)). Both types of patterns are derived from LPJmL simulations forced by HadGEM2-ES assuming rain-fed conditions and are expressed in percentage of change relative to the historical average yield at each grid point. Rows: Different crop types. Top panel shows relative differences,

bottom panel shows absolute differences. Analogous figures for irrigated conditions and for
370   different GGCMs are available as supplementary online material.

375
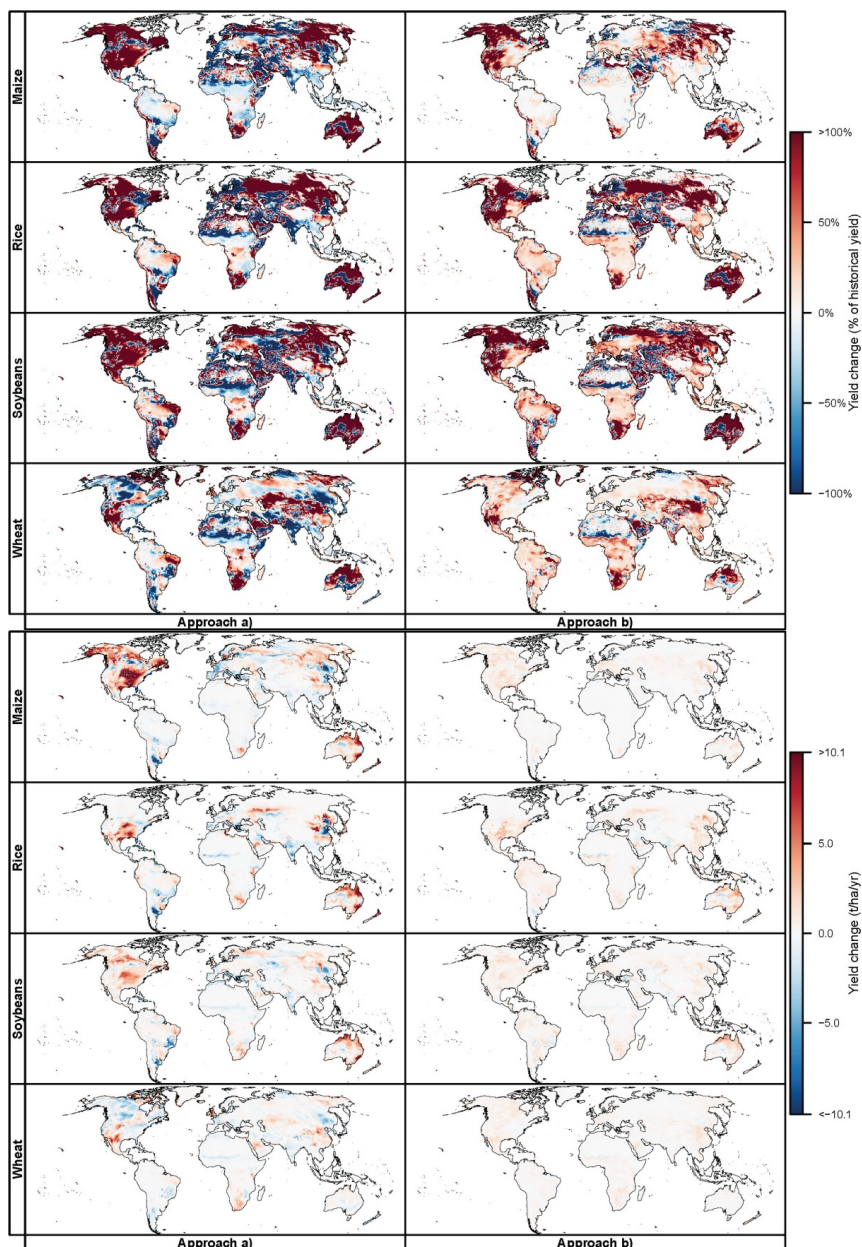
Figure 7. CO$_2$-induced yield changes at 2.5°C of global warming. Analogous to Fig. 6 but for the bin-specific CO$_2$ scaling coefficients a$_1$. **Rows:** Different crop types. Top panel shows relative differences, bottom panel shows absolute differences. Analogous figures for irrigated conditions and for different GGCMs are available as supplementary online material.

The two methods result in broadly similar patterns for the climate change-induced relative yield changes (i.e., excluding direct CO2 fertilization effects), with yield increases in the high latitudes

385 and decreases in the tropics and subtropics, broadly speaking (Fig. 6). However, the magnitudes of the changes are much larger with method (a) (Fig. 6, lower panel). Some regional differences also occur between the two methods, such as for rice where there is disagreement on the direction of yield changes in southeast Asia.

390 In relative terms (estimated climate change-induced yield change divided by simulated present-day yield), both methods show very large values of frequently alternating sign in areas such as the Arabian peninsula or the northern Sahel (Fig. 6, upper panel). This is likely due to the very low present-day yield potential in these regions, leading to division by values close to zero. In the regional evaluation of the different emulator methods below, we will account for these regional

395 differences in baseline yields by weighting potential yield changes by present-day growing areas.

The estimates of CO_2-induced yield changes also differ between the two methods (Figure 7). Method (b) results in a positive CO_2 effect in most regions, except for some low-yielding areas and the potentially important cases of soybean in southern and eastern South America, and rice in

400 north-west India and Pakistan, where it results in a negative effect of rising pCO_2 on yield. With method (a) on the other hand, areas of negative estimated CO_2 effect are much more widespread, and generally the magnitudes of the estimated CO_2 effect are again much larger than with method (b). As a preliminary conclusion, the results obtained with method (b) for the separate effects of climate change and pCO_2 change on potential yields appear more realistic than those

405 obtained with method (a).

410

4. Validation of three emulator approaches

Based on the climate-induced patterns (assuming fixed year 2000 levels of CO_2) of relative yield
415 changes and the associated within-bin relationship between CO_2 and crop yields identified in section 3, we propose the following two-step interpolation method to compute crop yield changes for any given pair of ΔGMT and pCO_2, using either of the above regression methods (a) or (b):

1. Linear interpolation between the temperature-specific, CO_2-adjusted yield patterns of
420   neighboring ΔGMT bins ($a_0(\Delta$GMT) from method (a) or $Y_{noCO2}(\Delta$GMT$) + a_0(\Delta$GMT$)$ from method (b)) to the desired ΔGMT value
2. Addition of the CO_2 pattern described by $a_1 * (CO_2 - 370ppm)$, where the pattern of scaling coefficients a_1 is also interpolated linearly between the scaling coefficients from neighboring temperature bins

425

The application of these two steps using regression method (a) will be called emulator approach (a); their application using regression method (b) will be called emulator approach (b). In a third, very basic emulator approach (c), crop yield change patterns for a given ΔGMT level are derived from an interpolation between the two neighboring ΔGMT bins' average patterns; where these

430   average patterns are derived from the RCP8.5 projections of the individual climate and crop model simulations accounting for the CO2 fertilization effect. E.g. to derive the crop yield change pattern for a global mean warming of 2.3°C:

$$\Delta Y\,(2.3°C) = (1 − \delta)\,<\Delta Y_{CO2}>_{2°C} + \delta\,<\Delta Y_{CO2}>_{2.5°C}$$

435    $$\delta = (2.3°C − 2°C)/(2.5°C − 2°C).$$

Using GGCM projections for the HadGEM2-ES climate input, we test which of the approaches, (a), (b) or (c), provides the best reproducibility for RCP2.6, RCP4.5, and RCP6.0 when estimates of the climate-induced and CO2-induced effects are based on RCP8.5 projections. While approach (b)

440   requires a pair of crop model simulations – one with time-varying pCO2 and one with fixed pCO2, approach (a) only requires the default simulations with time-varying pCO2. Approach (c) assumes that yield changes can be estimated using only ΔGMT as a predictor without consideration of the associated pCO2. Thus, a comparison of the three approaches could provide some important guidance regarding future crop model experiments required to allow for the proposed highly

445   efficient emulation of crop model simulations.
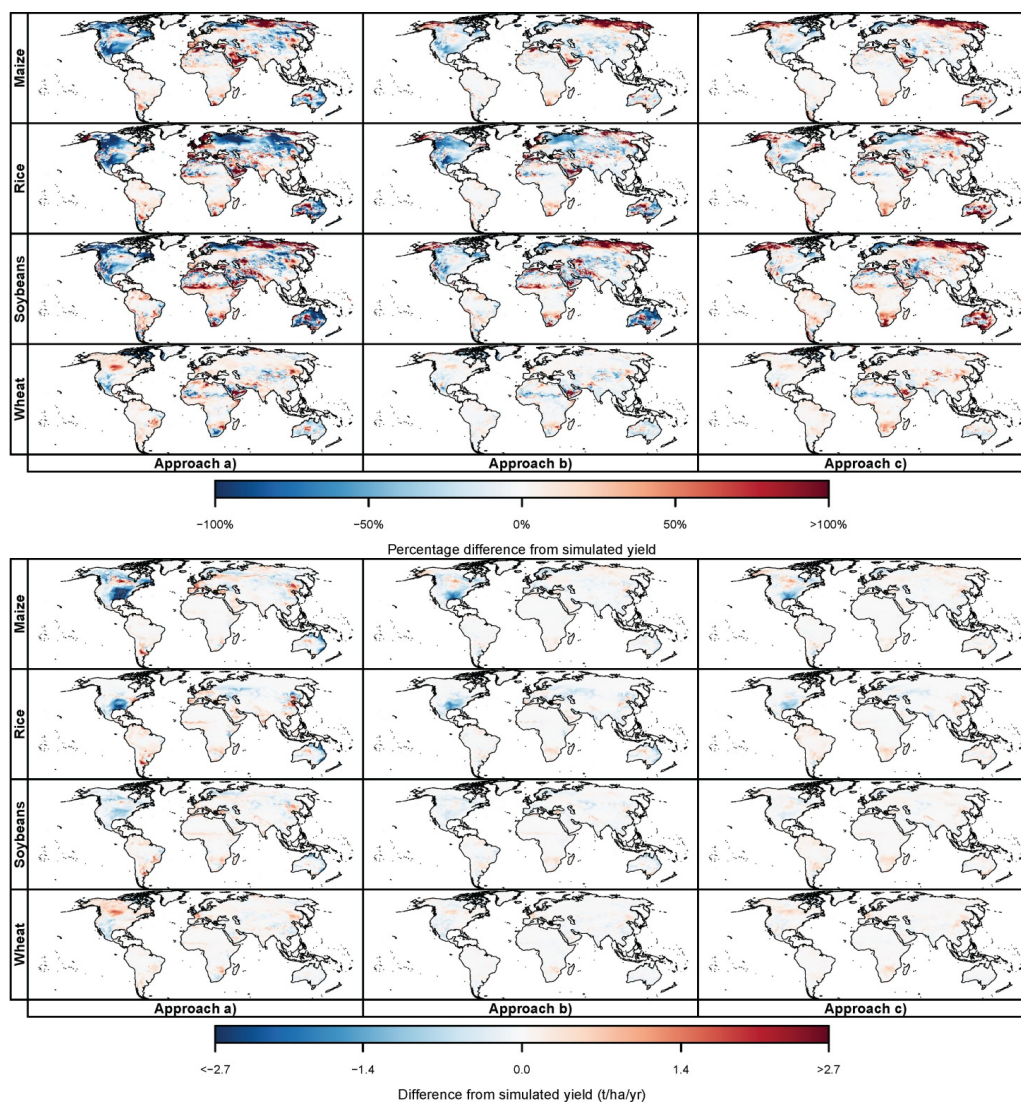
450

Figure 8. Validation of the three emulator approaches. Difference between the simulated yields (at a global mean warming of 2.5°C and a mean level of CO2 of 530 ppm as associated with RCP4.5) and the emulated yields based on approach (a) (left column), approach (b) (middle column), and approach (c) (right column). Top panel shows relative differences, bottom panel shows absolute differences. Analogous figures for irrigated conditions and for different GGCMs are available as supplementary online material.

455

460   Approach (a) generally leads to the largest differences relative to the simulated yield change (Fig.
8, left column). In particular Maize, rice, and soybean yields are underestimated for much of North
America, and overestimated in Europe and South America. Wheat yields are overestimated e.g. in
Canada. These discrepancies are mainly due to the climate-change effect estimated by approach
(a) (cf. Figure 6), whereas the CO2 fertilization effect even points in the opposite direction in many
465   of these regions (cf. Figure 7). In fact, we note again that approach (a) estimates the CO2
fertilization effect to be negative in some regions (Figure 7), which is not consistent with theory
and empirical evidence.

Approach (b) also leads to some substantial deviations from the potential yields simulated by
470   LPJmL, in percentage terms, mainly in the northern hemisphere and in Australia (Figure 8, top
panel, middle column). But large relative differences are mainly found outside the major growing
regions of the respective crop, in areas where absolute potential yields are low today.
Correspondingly, absolute differences between the LPJmL simulations and the emulator (b) are
modest (Figure 8, bottom panel, middle column). An important exception is the underestimation
475   of simulated maize and rice yields in southern North America. We note that LPJmL itself has
limitations in simulating yield variability in this region (Frieler et al., 2017).

Finally, approach (c) leads to a similar pattern of deviations from the simulated yield potential as
approach (b), but with a slightly smaller magnitude (Figure 8, right column). Thus, considering
480   overall performance at the grid point level for this particular case (2.5°C warming under RCP4.5),
the simple emulator approach (c) produces results which are closest to the LPJmL simulation.

To get a more comprehensive indicator of the performance of the emulator we use all three
approaches to reproduce the changes in crop production under RCP2.6, RCP4.5, and RCP6.0, as
485   derived for 10 large scale world regions (cf. Figure 2 in (Lotze-Campen et al., 2008) for a map of
the regions), assuming fixed year-2000 land use and irrigation patterns. Compared to potential
yields, using production gives less weight to areas where a crop is not currently grown. The
climate-induced and CO2-induced patterns of change were derived from RCP8.5; and we used the
RMSE between the relative changes in crop production derived from the original simulations and
490   their emulated counterparts across the other three scenarios as a measure of the performance of
the emulator.

Of the two approaches that estimate warming and CO_2-induced effects separately, approach (b)
generally provides a better performance than approach (a) (see Figure 9 for LPJmL; Table 1 and
495   supplementary online information for all crop models). Performance of all emulator approaches
varies substantially between regions. There are also considerable differences between crop
models. For LPJmL, emulator approach (b) generally provides marginally better performance for
many regions than approach (c) when emulating RCP2.6 and RCP4.5. This advantage of approach
(b) is not found in the other crop models. Taking into account that approach (b) requires additional
500   crop model simulations with fixed CO_2, the very basic interpolation approach (c) may provide the
best compromise between emulator performance and complexity.

While none of the emulators is expected to capture the relatively large inter-annual variability of simulated yield changes, approach (c) allows to emulate the regionally averaged response of the
505   process-based crop models to climate forcing estimated for RCP2.6, RCP4.5, and RCP6.0 (Fig. 10 for maize yields from LPJmL forced by HadGEM2-ES; analogous figures for other combinations are available as supplementary online material). Note though that the average deviation between emulated and simulated yields over the full 95-year time series is sometimes larger than the simulated yield change in 2091 − 2099, especially in the low warming scenarios (marked by red
510   crosses in Fig. 9).
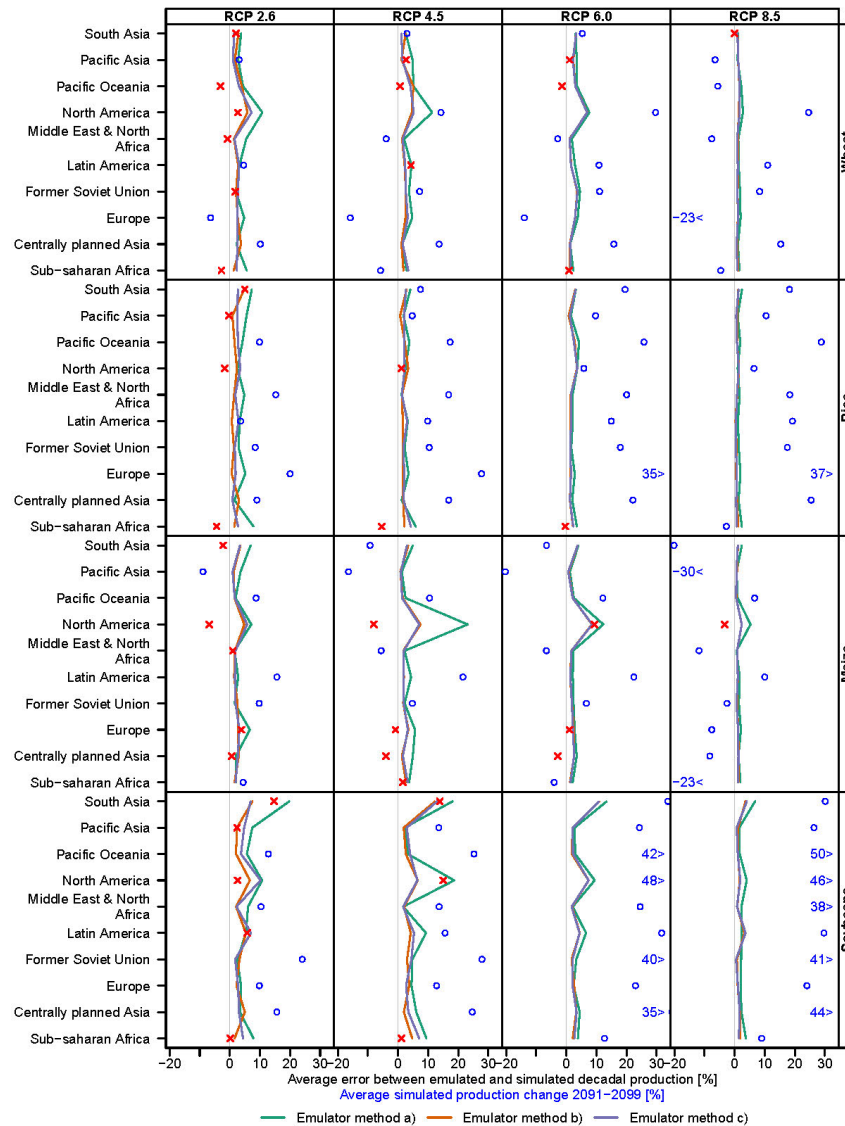
Fig. 9. Average root mean square deviation between emulated and simulated regional decadal production (yields weighted by year-2000 growing areas, combined for irrigated and rainfed crops)
515   for LPJmL forced by HadGEM2-ES climate projections. The emulator was built on the RCP8.5

projections and used to reproduce yield changes in all four RCPs. For comparison, blue circles illustrate the average simulated yield change for 2091 – 2099 (same horizontal axis; where the deviation between emulated and simulated yields is larger than the simulated yield change, red crosses are shown instead of blue circles).

520

Table 1. Average root mean square deviation between emulated and simulated decadal production (as in Fig. 9) in the largest producing region of each crop, for all five crop models forced by HadGEM2-ES climate projections. Average over all four RCPs. The values for all combinations of models, crops, and regions, and separately for each RCP, can be found in the supplementary online material.

method	Wheat, Europe			Rice, South Asia			Maize, North America			Soy, Latin America		
	a	b	c	a	b	c	a	b	c	a	b	c
GEPIC	2.159	1.250	1.396	6.941	3.321	3.266	19.091	10.310	9.664	5.001	2.638	2.858
LPJ-GUESS	2.579	2.348	2.486	5.026	2.614	4.517	10.034	7.029	6.866	3.749	3.003	2.691
LPJmL	3.814	2.272	2.415	4.247	2.954	2.409	11.954	5.783	5.950	5.869	4.313	5.084
pDSSAT	4.863	4.495	4.392	6.483	5.232	4.971	12.752	8.065	7.984	8.276	5.358	4.809
PEGASUS	8.125	4.923	5.324	n.a.	n.a.	n.a.	14.097	11.829	11.825	11.542	6.370	7.182
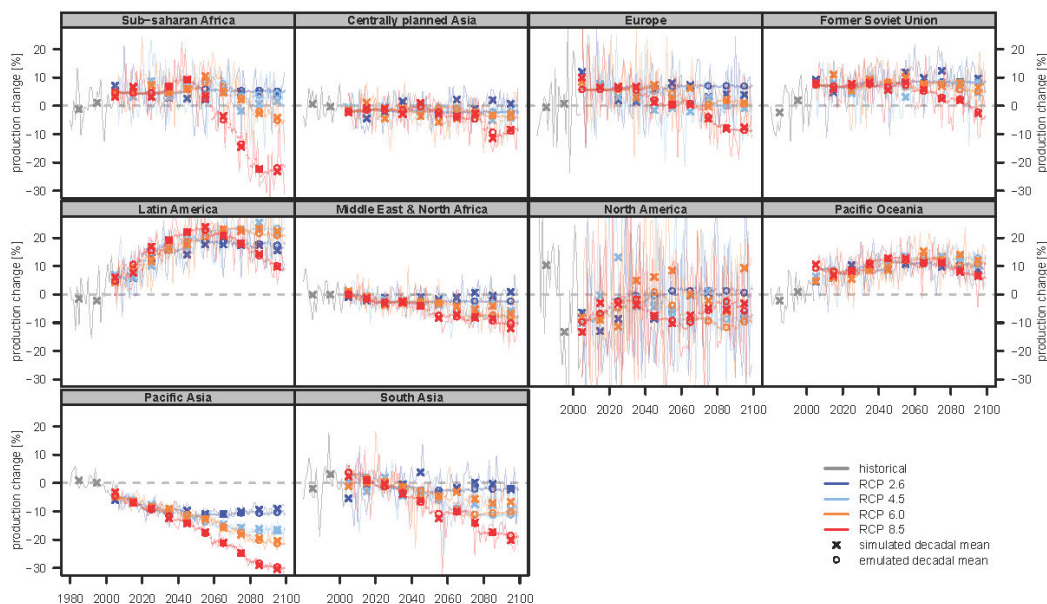
525 **Fig. 10.** Comparison of simulated and emulated time series of regionally averaged crop production changes for LPJmL forced by HadGEM2-ES climate projections. Regional averages are calculated based on fixed present day land use and irrigation patterns. Results are shown for Maize and emulator approach (c).

530

5. Increases in Regional Crop Yield Variance

In addition to estimating the yield changes associated with a rise in average temperature, it is important to consider the implications of rising variance. Climate change is expected to increase not only the average temperature, but to impact the variance of temperature and precipitation, including an increase in the frequency and duration of extreme events. For this reason, when deriving simplified relationships between potential yields and global climate change, it is crucial to account not only for the mean effects of rising temperature, but also their concurrent implications for crop yield variance. Interannual yield variance can be computed for the same 0.5° C warming bins as used above for the average yields, which we do here for all major crops under the "no irrigation" scenario. To account for the variability across scenarios and models which is attributable to direct CO2 effects, the RCP-GCM-GGCM specific mean is subtracted at each 0.5°C ΔGMT step. The variance of the adjusted yields is then compared to the variance of the same GCM-GGCM combination over the historical (1980-2010) period.

The global figures show broadly similar patterns across all four crops: Increases in yield variability in much of the northern hemisphere, particularly in North America, central Asia, and China; as well as in the southern mid-latitudes (Figure 11 for 2.5°C). A majority of model combination projects decreasing variability in tropical regions as well as parts of Eastern Europe; but nowhere do more than 75% of the model combinations agree on a decrease in variability. In several instances increased variability occurs in highly productive regions such as in China for rice and the US, Brazil, and Argentina for soy. Wheat also has an increased variability in more than 75% of the crop model simulations over the highly productive regions in China and the U.S. Such an increase in variability, if realized, could manifest as impacts on the price, whose volatility is tightly linked to rapid changes in supply (Gilbert and Morgan 2010).
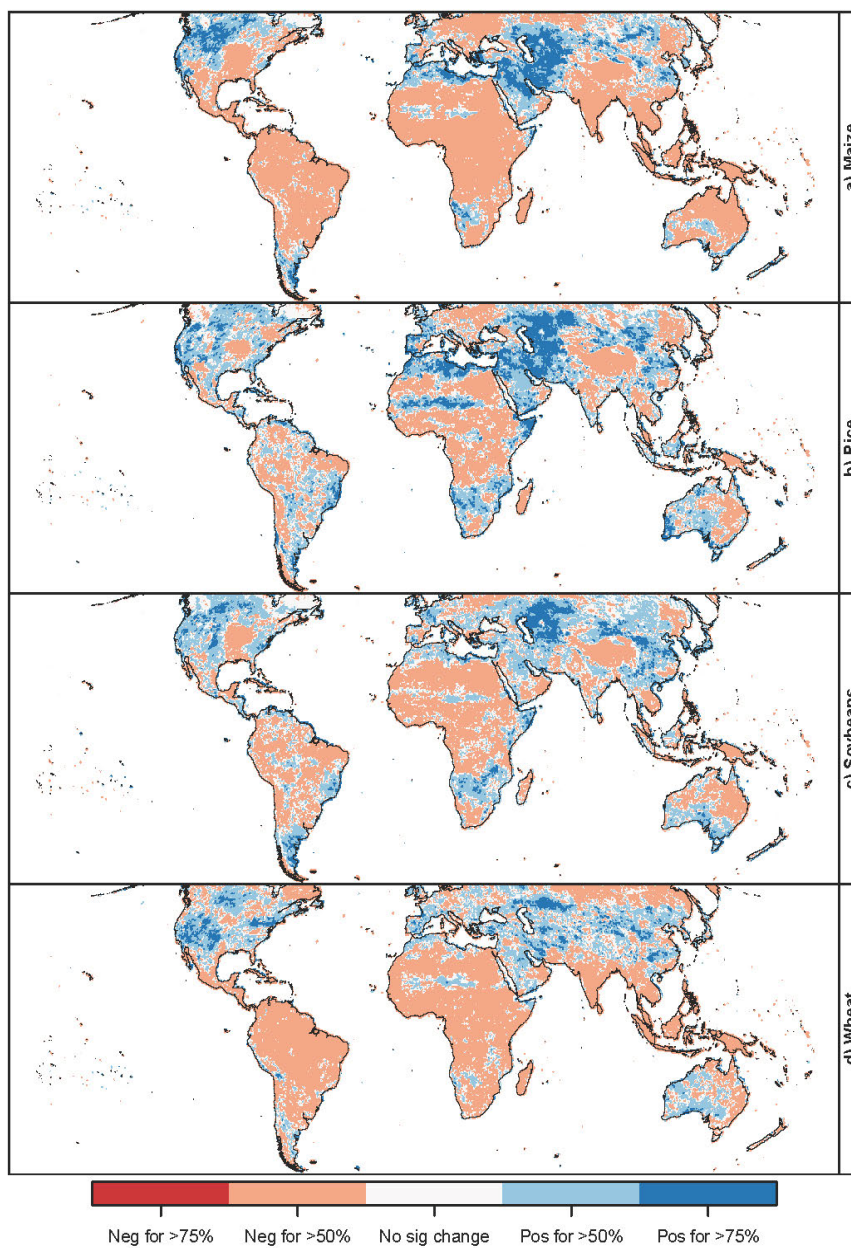
Fig 11. Percentage of crop model simulations indicating an increase (blue) or decrease (red) in
yield variance of greater than 5% at each grid point at 2.5°C warming scenario as compared to the
historic period for a) maize, b) rice, c) soy, and d) wheat.

6. Summary

570

Evaluating the impacts of climate change at different levels of global warming, and thus evaluating mitigation targets, requires a functional link between ΔGMT and regional impacts. Here we have shown that changes in crop yields, as simulated by gridded global crop models, can be
575 reconstructed based on ΔGMT, with some limitations. The small spread of simulated yield change across the RCP scenarios as compared to the GCMs and impact models implies that projected impacts at different ΔGMT levels are not substantially dependent on the choice of emissions pathway.

580 We have tested three different approaches for emulating crop yield changes simulated by GGCMs, two of which include pCO2 as an additional predictor. An approach (a) attributing the variation within an individual ΔGMT bin of a simulation with varying pCO2 solely to the change in pCO2 shows the poorest overall performance. An approach (b) based on the difference between runs with and without direct CO2 fertilization effects performs similarly well as a simple approach (c)
585 using only ΔGMT as a single predictor. For local (grid level) crop yields, approach (c) performs slightly better than approach (b) for the LPJmL GGCM. On the other hand, for yield changes weighted by actual growing areas and irrigation patterns and aggregated over large regions (i.e., regional production), approach (b) slightly outperforms approach (c) in reproducing changes under low-warming RCPs. Considering the added complexity in approach (b) compared to (c), the simple
590 approach (c) appears in general preferable. This suggests that simplified predictions of large-scale agriculture yields may not require additional crop model simulations with CO_2 levels held at a historical level.

The impact model ensemble available with ISIMIP data also indicates that the variability of crop
595 yields is projected to increase in conjunction with increasing ΔGMT in many important regions for the four major staple crops. Such a hike in yield volatility could have significant policy implications by affecting food prices and supplies.

The scalability of each component (mean yields and yield variability) is conducive to the
600 development of predictor functions relating ΔGMT, or other aggregate climate variable readily available from simplified climate models (such as pCO_2) to regional or global mean crop yield impacts. This lays the groundwork for a further exploration of the economic impacts of climate change encountered at target warming levels or over policy relevant regions.

Data availability
605 The coefficients estimated with equations (1) and (2) are available in the supplementary online material, along with supplementary figures and RMSE estimates, at https://cloud.pik-potsdam.de/index.php/s/5J8vDoQvycH2nuZ. The GGCM simulations that the analysis in this paper is based on are available through https://esg.pik-potsdam.de/search/isimip-ft/, with additional
610 documentation available on the ISIMIP website https://www.isimip.org/outputdata/caveats-fast-track/.

Acknowledgments

This work was supported within the framework of the Leibniz Competition (SAW-2013 PIK-5) and
615   by the EU FP7 HELIX project (grant no. 603864).

References

620   Blanc, É. (2017). Statistical emulators of maize, rice, soybean and wheat yields from global gridded
      crop models. *Agricultural and Forest Meteorology*, *236*, 145–161.
      http://doi.org/10.1016/j.agrformet.2016.12.022

Carter, T. R., Hulme, M., & Lal, M. (2007). General guidelines on the use of scenario data for
      climate impact and adaptation assessment.

Challinor A J and Wheeler T R 2008 Crop yield reduction in the tropics under climate change:
625   Processes and uncertainties *Agric. For. Meteorol.* **148** 343–56

Darwin R and Kennedy D 2000 Economic Effects of CO2 Fertilization of Crops: Transforming
      Changes in Yield into Changes in Supply *Environ. Model. Assess.* **5** 157–68

Eyshi Rezaei E, Gaiser T, Siebert S, Sultan B and Ewert F 2014 Combined impacts of climate
      and nutrient fertilization on yields of pearl millet in Niger *Eur. J. Agron.* **55** 77–88

630   FAO. (2007). *FertiSTAT - Fertilizer Use Statistics*. Rome: Food and Agricultural Organization of
      the UN.

Frieler, K., Arneth, A., Balkovic, J., Chryssanthacopoulos, J., Deryng, D., Elliott, J., Folberth,
      C., … Levermann, A. (2017). Understanding the weather-signal in national crop-yield
      variability. *Earth's Future*, *accepted*.

635   Frieler K, Levermann a., Elliott J, Heinke J, Arneth a., Bierkens M F P, Ciais P, Clark D B, Deryng
      D, Döll P, Falloon P, Fekete B, Folberth C, Friend a. D, Gellhorn C, Gosling S N, Haddeland I,
      Khabarov N, Lomas M, Masaki Y, Nishina K, Neumann K, Oki T, Pavlick R, Ruane a. C,
      Schmid E, Schmitz C, Stacke T, Stehfest E, Tang Q, Wisser D, Huber V, Piontek F,
      Warszawski L, Schewe J, Lotze-Campen H and Schellnhuber H J 2015 A framework for the
640   cross-sectoral integration of multi-model impact projections: land use decisions under
      climate impacts uncertainties *Earth Syst. Dyn.* **6** 447–60 Online: http://www.earth-syst-
      dynam.net/6/447/2015/

Frieler K, Meinshausen M, Mengel M, Braun N and Hare W 2012 A scaling approach to
      probabilistic assessment of regional climate change *J. Clim.* **25** 3117–44

645   Gilbert C L and Morgan C W 2010 Food price volatility. *Philos. Trans. R. Soc. Lond. B. Biol. Sci.*
      365 3023–34

Giorgi F 2008 A simple equation for regional climate change and associated uncertainty *J.
      Clim.* **21** 1589–604

Heinke J, Ostberg S, Schaphoff S, Frieler K, Müller C, Gerten D, Meinshausen M and Lucht W

650   2013 A new climate dataset for systematic assessments of climate change impacts as a
       function of global warming *Geosci. Model Dev.* **6** 1689–703

       Hempel S, Frieler K, Warszawski L, Schewe J and Piontek F 2013 A trend-preserving bias
       correction -- the ISI-MIP approach *ESD* **4** 219–36

       IFA. (2002). *Fertilizer Use by Crop*, *5th edn*. Rome.

655   Jaggard K W, Qi A and Ober E S 2010 Possible changes to arable crop yields by 2050. *Philos.
       Trans. R. Soc. Lond. B. Biol. Sci.* **365** 2835–51

       Kimball B A 1983 Carbon Dioxide and Agricultural Yield: An Assemblage and Analysis of 430
       Prior Observations1 *Agron. J.* **75** 779

       Lindeskog, M., Arneth, A., Bondeau, A., Waha, K., Schurgers, G., Olin, S., & Smith, B. (2013).
660   Effects of crop phenology and management on the terrestrial carbon cycle: case study for
       Africa. *Earth Syst. Dynam. Discuss.*, *4*(2), 235–278.

       Lindeskog, M., Arneth, A., Bondeau, A., Waha, K., Seaquist, J., Olin, S., & Smith, B. (2013).
       Implications of accounting for land use in simulations of ecosystem carbon cycling in Africa.
       Earth System Dynamics, *4*(2), 385–407. http://doi.org/10.5194/esd-4-385-2013

665   Lobell D B, Sibley A and Ivan Ortiz-Monasterio J 2012 Extreme heat effects on wheat
       senescence in India *Nat. Clim. Chang.* **2** 186–9

       Lotze-Campen, H., Müller, C., Bondeau, A., Rost, S., Popp, A., & Lucht, W. (2008). Global food
       demand, productivity growth, and the scarcity of land and water resources: a spatially explicit
       mathematical programming approach. *Agricultural Economics*. http://doi.org/10.1111/j.1574-
670   0862.2008.00336.x

       Meinshausen M, Smith S J, Calvin K, Daniel J S, Kainuma M L T, Lamarque J, Matsumoto K,
       Montzka S A, Raper S C B, Riahi K, Thomson A, Velders G J M and van Vuuren D P P 2011
       The RCP greenhouse gas concentrations and their extensions from 1765 to 2300 *Clim.
       Change* **109** 213–41

675   Mendelsohn R, Basist A, Dinar A, Kurukulasuriya P and Williams C 2007 What explains
       agricultural performance: Climate normals or climate variance? *Clim. Change* **81** 85–99

       Mitchell T D 2003 Pattern Scaling. An Examination of the Accuracy of the Technique for
       Describing Future Climates *Clim. Change* **60** 217–42

       Müller C, Elliott J and Levermann A 2014 Food security: Fertilizing hidden hunger *Nat. Clim.
680   Chang.* **4** 540–1 Online: http://www.nature.com/doifinder/10.1038/nclimate2290

       Müller C and Robertson R D 2014 Projecting future crop productivity for global economic
       modeling *Agric. Econ. (United Kingdom)* **45** 37–50

       Nelson G C, van der Mensbrugghe D, Ahammad H, Blanc E, Calvin K, Hasegawa T, Havlik P,
       Heyhoe E, Kyle P, Lotze-Campen H, von Lampe M, Mason d'Croz D, van Meijl H, Müller C,
685   Reilly J, Robertson R, Sands R D, Schmitz C, Tabeau A, Takahashi K, Valin H and
       Willenbockel D 2014 Agriculture and climate change in global scenarios: Why don't the
       models agree *Agric. Econ. (United Kingdom)* **45** 85–101

Ostberg S, Lucht W, Schaphoff S and Gerten D 2013 Critical impacts of global warming on land ecosystems *Earth Syst. Dyn.* **4** 347–57

690 Parry M, Rosenzweig C and Livermore M 2005 Climate change, global food supply and risk of hunger. *Philos. Trans. R. Soc. Lond. B. Biol. Sci.* **360** 2125–38

Peng S, Huang J, Sheehy J E, Laza R C, Visperas R M, Zhong X, Centeno G S, Khush G S and Cassman K G 2004 Rice yields decline with higher night temperature from global warming. *Proc. Natl. Acad. Sci. U. S. A.* **101** 9971–5

695 Portmann F T, Siebert S and Döll P 2010 MIRCA2000—Global monthly irrigated and rainfed crop areas around the year 2000: A new high-resolution data set for agricultural and hydrological modeling *Global Biogeochem. Cycles* **24**

Ramankutty N, Foley J A, Norman J and McSweeney K 2002 The global distribution of cultivable lands: Current patterns and sensitivity to possible climate change *Glob. Ecol.*
700 *Biogeogr.* **11** 377–92

Rosenzweig C, Elliott J, Deryng D, Ruane A C, Müller C, Arneth A, Boote K J, Folberth C, Glotter M, Khabarov N, Neumann K, Piontek F, Pugh T a M, Schmid E, Stehfest E, Yang H and Jones J W 2014 Assessing agricultural risks of climate change in the 21st century in a global gridded crop model intercomparison. *Proc. Natl. Acad. Sci. U. S. A.* **111** 3268–73
705 Online:
http://www.pubmedcentral.nih.gov/articlerender.fcgi?artid=3948251&tool=pmcentrez&rendertype=abstract

Santer, B. D., Wigley, T. M. L., Schlesinger, M. E., & Mitchell, J. F. B. (1990). Developing climate scenarios from equilibrium GCM results. *Max-Planck-Institut Für Meteorologie Report*, *47*.

710 Schewe J, Heinke J, Gerten D, Haddeland I, Arnell N W, Clark D B, Dankers R, Eisner S, Fekete B M, Colón-González F J, Gosling S N, Kim H, Liu X, Masaki Y, Portmann F T, Satoh Y, Stacke T, Tang Q, Wada Y, Wisser D, Albrecht T, Frieler K, Piontek F, Warszawski L and Kabat P 2014 Multimodel assessment of water scarcity under climate change. *Proc. Natl. Acad. Sci. U. S. A.* **111** 3245–50 Online:
715 http://www.pubmedcentral.nih.gov/articlerender.fcgi?artid=3948304&tool=pmcentrez&rendertype=abstract

Schlenker W and Roberts M J 2009 Nonlinear temperature effects indicate severe damages to U.S. crop yields under climate change. *Proc. Natl. Acad. Sci. U. S. A.* **106** 15594–8

Smith P, Gregory P J, van Vuuren D, Obersteiner M, Havlík P, Rounsevell M, Woods J, Stehfest E
720 and Bellarby J 2010 Competition for land. *Philos. Trans. R. Soc. Lond. B. Biol. Sci.* **365** 2941–57

Solomon S, Plattner G-K, Knutti R and Friedlingstein P 2009 Irreversible climate change due to carbon dioxide emissions. *Proc. Natl. Acad. Sci. U. S. A.* **106** 1704–9

Stehfest E, van Vuuren D, Kram T, Bouwman L, Alkemade R, Bakkenes M, Biemans H,
725 Bouwman A, den Elzen M, Janse J, Lucas P, van Minnen J, Müller M and Prins A 2014 *Integrated Assessment of Global Environmental Change with IMAGE 3.0. Model description and policy applications* (The Hague: PBL Netherlands Environmental Assessment Agency)

Van der Velde M, Tubiello F N, Vrieling A and Bouraoui F 2012 Impacts of extreme weather on wheat and maize in France: Evaluating regional crop simulations against observed data *Clim. Change* **113** 751–65

Van Vuuren D P, Edmonds J, Kainuma M, Riahi K, Thomson A, Hibbard K, Hurtt G C, Kram T, Krey V, Lamarque J F, Masui T, Meinshausen M, Nakicenovic N, Smith S J and Rose S K 2011 The representative concentration pathways: An overview *Clim. Change* **109** 5–31

Waha, K., van Bussel, L., Müller, C., & Bondeau, A. (2012). Climate-driven simulation of global crop sowing dates. *Global Ecology and Biogeography*, *21*, 247–259.

Wang D, Heckathorn S a., Wang X and Philpott S M 2012 A meta-analysis of plant physiological and growth responses to temperature and elevated CO 2 *Oecologia* **169** 1–13

Warszawski, L., Frieler, K., Huber, V., Piontek, F., Serdeczny, O., & Schewe, J. (2013). The Inter-Sectoral Impact Model Intercomparison Project (ISI-MIP): Project framework. *Proceedings of the National Academy of Sciences of the United States of America*, 1–5. http://doi.org/10.1073/pnas.1312330110

Yin X 2013 Improving ecophysiological simulation models to predict the impact of elevated atmospheric CO2 concentration on crop productivity *Ann. Bot.* **112** 465–75

745